Table II. Mössbauer Parameters[a]

compd	temp, K	IS,[b] mm/s	QS, mm/s	Γ_h,[c] mm/s	Γ_l,[c] mm/s	I_h/I_l[d]
$Fe(dhe\text{-}dtc)_3 \cdot 3H_2O$	300	0.725	0.138	0.394	0.621	0.86
	78	0.842	0.251	0.253	0.463	0.66
		0.783	0.675	0.543	0.543	1.0
$Fe(dhe\text{-}dtc)_3$	300	0.620	0.716	0.553	0.507	0.82
	78	0.733	1.041	0.534	0.651	0.60

[a] Accurate up to ±0.016 mm/s. [b] Relative to SNP. [c] Γ_h and Γ_l are the full widths at half-height of the high- and low-energy lines, respectively. [d] I_h and I_l are the intensities of the high- and low-energy lines, respectively.

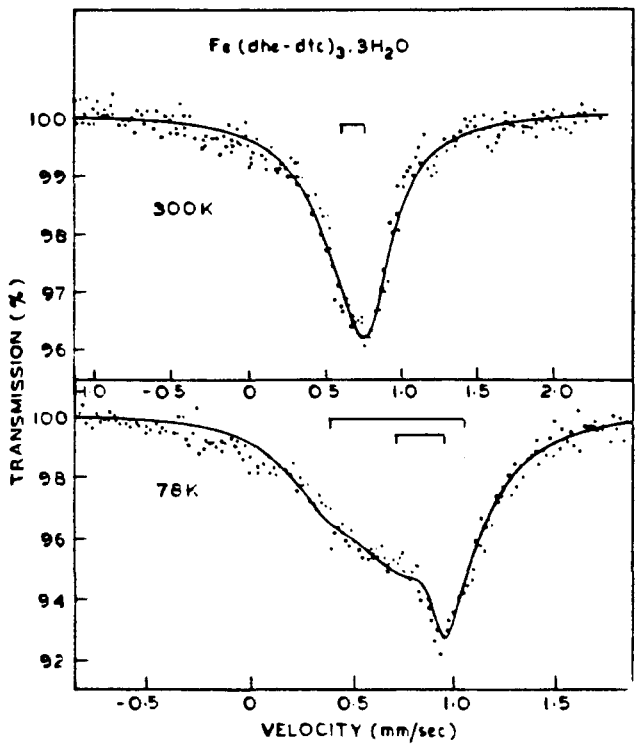

Figure 3. Mössbauer spectra of $Fe(dhe\text{-}dtc)_3 \cdot 3H_2O$.

those of the recently reported tris(methyl-*n*-butyldithiocarbamato)iron(III), which is largely in the high-spin state at room temperature (4.7 μ_B).[20]

The spectrum at liquid-nitrogen temperature is highly asymmetric (Figure 3). When the data were fitted for one quadrupole doublet, the results yielded unusually large line widths. Instead, the results could be quite successfully fitted for two quadrupole doublets. Mössbauer parameters for the inner doublet correspond to the high-spin state and those for the outer doublet to the low-spin state.[32] The isomer shift for the outer doublet is less positive than that of the inner doublet. It is well-known[33,34] that the low-spin iron(III) shows lower isomer shift values than the high-spin iron(III). Now, since the Mössbauer spectrum of the compound under discussion at liquid-nitrogen temperature shows more or less separate quadrupole doublets for high-spin and low-spin states, the $S = {}^1/_2 \rightleftharpoons S = {}^5/_2$ intersystem crossing rate in the solid state of the compound at 78 K has an upper limit of 10^7 s^{-1}, so that τ(low spin) and τ(high spin) are 10^{-7} s. This, to our knowledge, is the first report of separate Mössbauer quadrupole doublets for the two spin states in a tris(dithiocarbamato)iron(III) complex.

The higher rates of interconversion in tris(dialkyldithiocarbamato)iron(III) complexes have, in general, been attributed to the higher metal–ligand covalency and spin–orbit interaction.[4] It is interesting to observe here that these factors in $Fe(dhe\text{-}dtc)_3 \cdot 3H_2O$ and $Fe(dhe\text{-}dtc)_3$ differ to such an extent that distinctly different rates of interconversion result. Several iron(III) complexes with N,O-donor Schiff base ligands are also known to show distinct changes in the rates of spin-state interconversion by minor lattice alterations.[8-15] For example, the complex $[Fe(acen)(4\text{-}Mepy)_2]BPh_4$, where acen is *N*,*N*′-bis(1-methyl-3-oxobutylidene)ethylenediamine, shows rapid spin-state interconversion (on the Mössbauer time scale), while $[Fe(acen)(3,4\text{-}Me_2py)]BPh_4$ shows slow spin-state interconversion.[12-15] Similarly, spin-state interconversions in $[Fe(acpa)_2]BPh_4 \cdot H_2O$ and $[Fe(acpa)_2]PF_6 \cdot H_2O$, where Hacpa is *N*-(1-acetyl-2-propylidene)-2-pyridylmethylamine, are respectively rapid and slow on the Mössbauer time scale.[12-15] Also Hendrickson's[8] $[Fe(SalAPA)_2]ClO_4$ flips spins faster by 1 order of magnitude than does $[Fe(SalAEA)_2]ClO_4$.

Acknowledgment. Our grateful thanks are due to Professor S. Mitra of the Tata Institute of Fundamental Research, Bombay, India, who kindly provided the laboratory facilities for carrying out variable-temperature magnetic suceptibility measurements, and to the University Grants Commission, New Delhi, India, for awarding Research Fellowships to R.S. and C.P.

Registry No. I, 75074-70-3; $Fe(dhe\text{-}dtc)_3 \cdot 3H_2O$, 109467-79-0; $Fe(dhe\text{-}dtc)_3$, 24551-23-3; bis(hydroxyethyl)amine, 111-42-2; carbon disulfide, 75-15-0.

(33) Erickson, N. E. *Adv. Chem. Ser.* **1967**, *No. 68*, 86.
(34) Brady, P. R.; Duncan, J. F.; Mok, K. F. *Proc. R. Soc. London, A* **1965**, *287*, 343.

Contribution from the Instituto de Quimica, Universidade de Sao Paulo, Sao Paulo, SP, Brazil

Cyclic Voltammetry and Resonance Raman Studies of the (Pyridine-2-carbaldoxime)tetracyanoferrate(II) Complex: Evidence of a Nitroso–Oxime Equilibrium

Henrique E. Toma* and Paulo S. Santos

Received May 5, 1987

The nitroso–oxime equilibrium in coordination compounds provides an interesting example of a ligand reaction that has been little investigated up to the present time. In this study, by working with the (pyridine-2-carbaldoxime)tetracyanoferrate(II) complex, $[Fe(CN)_4pyCHNOH]^{2-}$, we have obtained electrochemical evidence of two species in equilibrium, as expected for a nitroso–oxime system. In order to elucidate this point, we have investigated the Raman spectra of the complexes, as well as of the (α-imino-2-picoline)tetracyanoferrate(II) complex, $[Fe(CN)_4pyCHNH]^{2-}$, for comparison purposes.

Raman spectroscopy has been a powerful technique in studies of complexes such as the iron(II) diimines,[1-3] because of the occurrence of resonance enhancement arising from the metal-to-ligand charge-transfer excitation. The vibrational modes that show enhanced Raman intensity are those vibronically active in the electronic transition, i.e. in the present case, those associated

(1) Clark, R. J. H.; Turtle, P. C.; Srommen, D. P.; Streusend, B.; Kincaid, J.; Nakamoto, K. *Inorg. Chem.* **1977**, *16*, 84.
(2) Batschelet, W. H.; Rose, N. J. *Inorg. Chem.* **1983**, *22*, 2078.
(3) Czernuszewicz, R. S.; Nakamoto, K.; Strommen, D. P. *Inorg. Chem.* **1980**, *19*, 793.

0020-1669/87/1326-3218$01.50/0

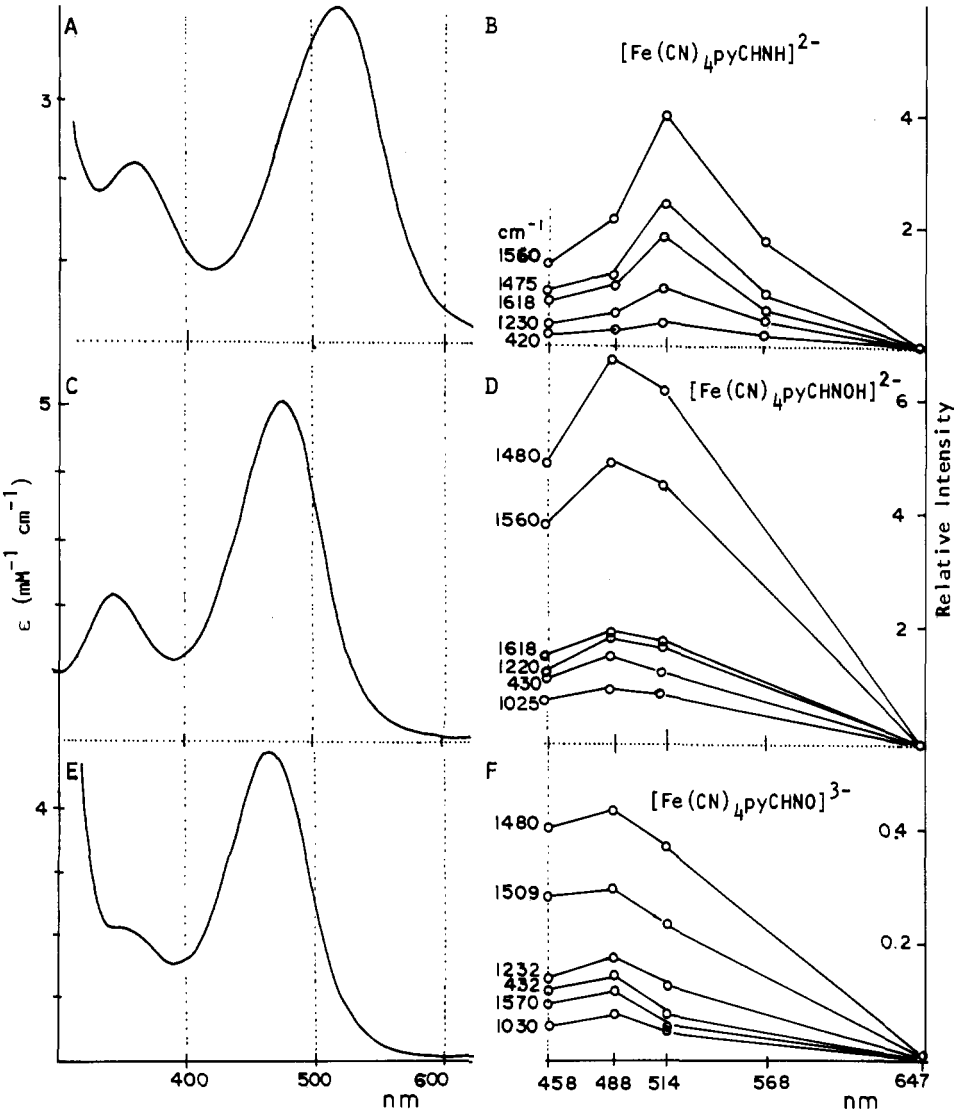

Figure 1. Absorption spectra in aqueous solution and excitation profiles for the (α-imino-2-picoline)tetracyanoferrate(II) complex (A, B) and the (pyridine-2-carbaldoxime)tetracyanoferrate(II) complex at pH 4.0 (C, D) and 10.0 (E, F).

with the Fe(II)–diimine chromophore.[2] For this reason, the changes in the chromophore group due to the oxime–nitroso conversion are expected to be readily detected in the resonance Raman spectra of the complexes.

Experimental Section

The $Na_2[Fe(CN)_4(pyCHNOH)]\cdot H_2O$ complex was prepared and purified according to published procedures for related compounds.[4] Anal. Calcd for $Na_2FeC_{10}N_6H_8O_2$: C, 34.71; N, 24.27; H, 2.33. Found: C, 35.0; N, 23.5; H, 2.0. The disodium (α-imino-2-pyridine)tetracyanoferrate(II) complex was prepared in a previous work[5] by the autoxidation of the corresponding α-amino-2-pyridine derivative. The crystalline sample employed in this work was kindly supplied by Dr. N. M. Iha.

Cyclic voltammetry measurements were carried out with a Princeton Applied Research instrument, consisting of a Model 173 potentiostat and a Model 175 universal programmer. A platinum electrode was employed for the measurements, along with the conventional Luggin capillary with the Ag/AgCl (1 M KCl) reference electrode. The auxiliary electrode was a platinum wire dipped into the electrolyte solution (0.5 M KCl) in a small compartment separated from the working solution by a fine glass frit. The temperature for all experiments was 25 °C. The measured potentials were converted to the normal hydrogen electrode (NHE) scale by adding 0.222 V.

The electronic spectra of the complexes were recorded on a Cary 17 or a Hewlett-Packard 8451 diode array spectrophotometer. Resonance Raman (RR) spectra were recorded on a Jarrell-Ash instrument, using Spectra-Physics argon and krypton ion lasers. The measurements were carried out in aqueous solution, containing sodium sulfate (0.2 M), with use of a spinning cell. The relative intensities were measured as peak heights relative to the sulfate Raman band at 980 cm^{-1}.

Results and Discussion

The electronic spectra of the $[Fe(CN)_4pyCHNOH]^{2-}$ complex (Figure 1) consist of two strong absorption bands at 473 nm (ϵ = 5100 M^{-1} cm^{-1}) and 347 nm (ϵ = 2300 M^{-1} cm^{-1}), associated with charge-transfer transitions from the metal $d(\pi)$ orbitals to the pyCHNOH $p(\pi^*_1)$ and $p(\pi^*_2)$ acceptor orbitals. Similar bands have been observed[5] for the $[Fe(CN)_4pyCHNH]^{2-}$ complex, at 515 and 360 nm, respectively. Above pH 10, the visible absorption band of the oxime complex is shifted to 465 nm (ϵ = 4800 M^{-1} cm^{-1}).

Cyclic voltammograms of the $[Fe(CN)_4pyCHNOH]^{2-}$ complex, measured at several pHs, are shown in Figure 2. Below pH 7 the voltammograms consist of a single wave associated with oxidation of the oxime complex. The voltammograms can be accurately fitted by the theoretical equation[6] for a reversible monoelectronic charge-transfer process with $E_{1/2}(Fe^{II/III})$ = 0.657 V vs. NHE and a diffusion coefficient of 6.0×10^{-6} cm^2 s^{-1}. Above pH 7, there is a systematic decrease in the peak currents for the oxime complex and a concomitant growing of a new, reversible wave, with $E_{1/2}(Fe^{II/III})$ = 0.387 V. The process involved is

(4) Goto, M.; Takeshita, M.; Sakai, T. *Inorg. Chem.* **1978**, *17*, 314.
(5) Toma, H. E.; Ferreira, A. M. C.; Iha, N. Y. M. *Nouv. J. Chim.* **1985**, *9*, 473.
(6) Nicholson, R. S.; Shain, I. *Anal. Chem.* **1964**, *36*, 706.

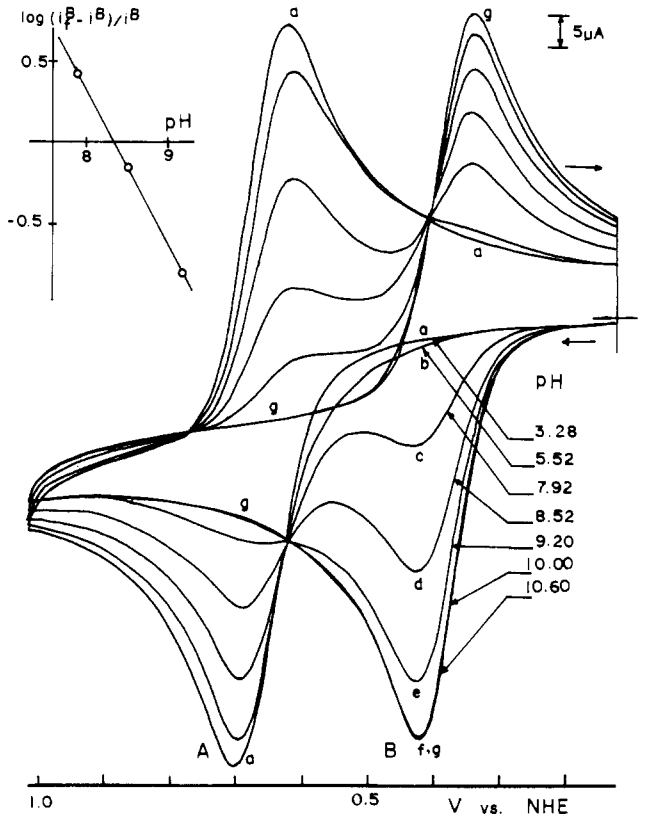

Figure 2. Cyclic voltammograms of the (pyridine-2-carbaldoxime)-tetracyanoferrate(II) complex (5 mM), measured at several pHs (25 °C, [KCl] = 0.5 M, potential scan rate 50 mV s^{-1}), and the linear logarithmic plot (inset) of the ratio of anodic peak currents at 0.42 V vs. pH, used to evaluate pK_a.

completely reversible (Figure 2) and can be ascribed to the equilibrium

$$\underset{A}{[(CN)_4Fe(pyCHNOH)]^{2-}} \rightleftharpoons \underset{B}{[(CN)_4Fe(pyCHNO)]^{3-}} + H^+ \quad (1)$$

The equilibrium constant can be readily evaluated from eq 2, where $i_f(B)$ is the anodic peak current of species B above pH 10.

$$pH = pK_a - \log([A]/[B]) = pK_a - \log((i_f(B) - i(B))/i(B)) \quad (2)$$

The experimental plot is shown as an insert in Figure 2. The linear behavior with a slope of unity is consistent with eq 2. At the intercept with the ordinate axis, pH = pK_a = 8.35 ± 0.05 (25 °C, 0.1 M KCl).

Measurements carried out at pH 7–9 as a function of the potential scan rates (10–200 mV s^{-1}) have shown that the rates of conversion from A to B are quite slow ($k < 0.1$ s), in contrast to the case for most acid–base reactions, and have no influence in the shape of the cyclic voltammograms. On the other hand, the difference of 270 mV in the redox potentials of species A and B is quite large, indicating that the loss of a proton from the oxime group leads to pronounced structural changes in the complex. In order to evaluate this point, we obtained the resonance Raman spectra of the complexes.

Typical Raman spectra for the $[Fe(CN)_4pyCHNOH]^{2-}$ complex at pH 4 and 10 are shown in Figure 3, in comparison to the spectrum of the $[Fe(CN)_4pyCHNH]^{2-}$ complex.

The α-imino-2-picoline complex exhibits excitation profiles that follow very closely the visible absorption band at 515 nm, associated with a metal-to-diimine charge-transfer transition[7] (Figure 1B). The spectra are quite similar to those previously reported by Batschelet and Rose,[2] for the tris(α-(methylimino)-2-

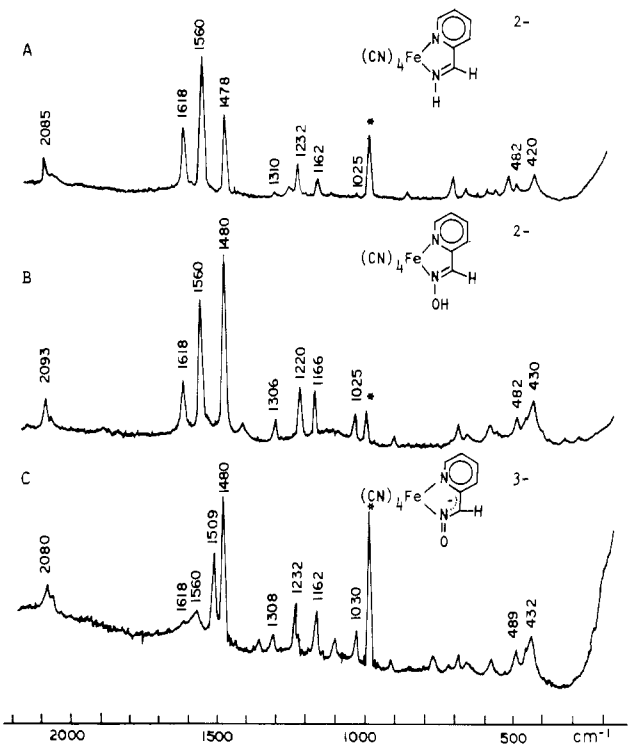

Figure 3. Resonance Raman spectra of the (α-imino-2-picoline)- (A) and (pyridine-2-carbaldoxime)tetracyanoferrate(II) complexes (B, C) (1 mM) in aqueous solution, showing the oxime form (B) at pH 4.0 (0.01 M acetate buffer) and the nitroso form (C) at pH 10.0 (0.01 M carbonate buffer) (λ_{ex} = 488 nm, $[Na_2SO_4]$ = 0.2 M, reference peak marked with an asterisk).

picoline)iron(II) complex, which exhibits a strong enhancement of the vibrational bands of the iron–diimine chromophore. Accordingly, the strong peak at 1618 cm^{-1} in Figure 3A has been ascribed[2] to the C=N stretch. The peak at 1556 cm^{-1} has also been observed in 2,2′-bipyridyl.[8] Normal-coordinate analysis has shown that the peak involves the CN and CC stretching vibrations of the pyridine ring.[8] This peak is quite enhanced, indicating a strong coupling of the pyridyl group with the imine moiety in the iron(II)–diimine chromophore. The strong peak at 1478 cm^{-1}, and the less intense peaks at 1448 and 1310 cm^{-1}, are also characteristic of the pyridyl group, involving a mixture of CC and CN stretch and HCC and HCN deformation vibrations.[8] The peak of medium intensity at 1232 cm^{-1} is probably associated with the CC stretching in the diimine chromophore. The weak peaks at 1162, 1025, and 860 cm^{-1} are in a region characteristic of in-plane HC bending, ring breathing, and out-of-plane HC bending vibrations, respectively, of aromatic molecules, while the peaks at 700 and 652 cm^{-1} are close to the CC and CN torsional modes, observed in the 2,2′-bipyridyl ligand.[8] In iron(II)–diimine complexes, the Fe–N stretching has been located[2] around 480 cm^{-1}, corresponding to the peak observed in this work at 482 cm^{-1}. The remaining peak at 420 cm^{-1} is strongly enhanced and can be tentatively assigned to the Fe–N(py) stretching mode. The vibrational bands characteristic of the cyanoferrate(II) moiety occur at 2085 and 2056 cm^{-1} (cyanide ion stretching) and 580 cm^{-1} (FeCN bending).

The RR spectra of the oxime complex below pH 7 are quite similar to those of the α-imino-2-picoline analogue, as one can see in Figure 3B. The excitation profiles follow very closely the visible absorption band, as shown in Figure 1D. Analogously, the vibrational peaks associated with the iron(II)–diimine chromophore at 1618 and 1560 cm^{-1} are strongly enhanced, as well as the pyridine band at 1480 cm^{-1}. The remaining bands are observed at the following positions (cm^{-1}): 2093, 2070 (cyanide ion stretching); 1412, 1306, 1220 (CC, CN stretching + HC bending);

(7) Krumholz, P. *Struct. Bonding (Berlin)* **1971**, *9*, 139.

(8) Strukl, J. S.; Walter, J. L. *Spectrochim. Acta, Part A* **1971**, *27A*, 209.

1166 (in-plane CH bending); 1025 (ring breathing); 895 (out-of-plane CH bending); 680, 650 (CC, CN torsion); 575 (FeCN bending); 482 (FeN stretching); 430 (Fe(py) stretching).

Above pH 7, the vibrational peaks associated with the iron(II)–diimine chromophore at 1618 and 1560 cm^{-1} decrease dramatically in intensity, as one can see in Figure 3C. A new, strongly enhanced peak grows at 1509 cm^{-1}, while the pyridine vibrations remain practically unchanged at 1480, 1308, 1232, 1162, 1030, 910, and 683 cm^{-1}. The excitation profiles also follow very closely the visible absorption spectra, as shown in Figure 1C. The complete decay of the characteristic diimine vibrational bands at pH 10 implies that the deprotonation of the oxime group has a pronounced effect on the conjugated chromophore. On the other hand, the new peak at 1509 cm^{-1} is in the range of 1570–1495 cm^{-1} characteristic of the N=O stretching vibration in aromatic and aliphatic nitroso compounds.[9]

Therefore, the RR spectrum of the oxime complex at pH 10 is consistent with the formation of a nitroso species. Nitroso complexes have also been detected[10] in the addition reactions of acetylpyridines to the nitrosyl ligand in the nitroprusside complex, $[Fe(CN)_5NO]^{2-}$. In these systems, a NO stretching peak has been observed around 1500 cm^{-1}. When the pH is lowered, oximes have been isolated in a high yield.

Acknowledgment. We thank the FAPESP, CNPq, and FINEP for financial support.

Registry No. $[Fe(CN)_4pyCHNOH]^{2-}$, 109585-62-8; $[Fe(CN)_4pyCHNO]^{3-}$, 109585-63-9; $[Fe(CN)_4pyCHNH]^{2-}$, 91730-48-2.

(9) Bellamy, L. J. *The Infra-red Spectra of Complex Molecules*, 3rd ed.; Chapman and Hall: London, 1975; p 340.
(10) Iha, N. Y. M.; Toma, H. *Inorg. Chim. Acta* **1984**, *71*, 181.

Contribution from the Department of Chemistry and Ames Laboratory,[1] Iowa State University, Ames, Iowa 50011

Effect of Ligand Geometry on ^{59}Co NMR Relaxation in Hexakis(phosphite)cobalt(III) Complexes

Steven M. Socol,* Serge Lacelle,*[2] and John G. Verkade

Received September 26, 1986

Cobalt-59 NMR spectroscopy has been shown to be a useful probe of the static and dynamic properties of octahedral cobalt(III) complexes.[3] Recently we described how ^{59}Co NMR can be used to quantify the ligand field in complexes of the type $[CoL_6]^{3+}$ for a series of phosphorus donor ligands L having different steric and electronic properties.[4,5] In these complexes, ^{59}Co–^{31}P spin–spin couplings were observed in the ^{59}Co NMR spectra only for complexes of phosphite ligands having 3-fold symmetry or chelating diphosphonite ligands possessing 2-fold symmetry. This result suggested that the geometry of the ligands influences the relaxation of the ^{59}Co nucleus. It therefore became of interest to measure the longitudinal relaxation of several of these complexes to determine the extent of such an effect.

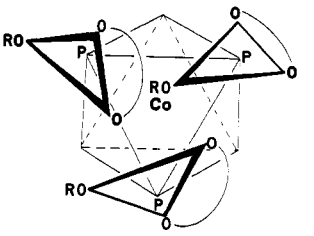

Figure 1. Schematic representation of the packing of monocyclic phosphite ester ligands around the octahedral Co^{3+} ion in one of the diastereomers of the $[CoL_6]^{3+}$ complex. The triangle in each ligand depicts the plane of the three esteratic oxygens while the curve denotes the ring carbons. The phosphorus atom is below the triangular plane. In the other diastereomer, the ligands around the bottom triangular face are rotated by 180° around the P–Co bonds.

Some ^{59}Co T_1 studies have been reported.[6-13] Since the ^{59}Co nucleus is spin $^7/_2$ and has a moderately large quadrupole moment, the longitudinal and transverse relaxation times of the magnetization of the ^{59}Co nucleus are expected to be dominated by the interaction of the nuclear electric quadrupole moment with fluctuating electric field gradients (quadrupole relaxation).[9,12] In the extreme narrowing limit with an axial electric field gradient at the quadrupolar nucleus, the quadrupolar relaxation rate, R_q, is given by

$$R_q = \left(\frac{3}{40}\right)\frac{(2I+3)}{I^2(2I-1)}\left(\frac{e^2Qq}{\hbar}\right)^2 \tau_E \qquad (1)$$

where eQ is the nuclear quadrupole moment, τ_E is the correlation time for the reorientation for the electric field gradient, eq, at the observed nucleus, and the rest of the symbols have their usual meaning.[9,14] Recently it has been reported that ^{59}Co NMR relaxation times shorten and line widths broaden with increasing applied field strength for six-coordinate cobalt(III) complexes of low symmetry, suggesting that chemical shift anisotropy also makes a contribution to the relaxation in these complexes.[6]

Here we show that (1) T_1 of ^{59}Co in phosphite ester complexes of the type $[CoL_6]^{3+}$ decreases when reducing the symmetry of the ligands, (2) the variation in the ^{59}Co T_1 values is not due to differences in rotational correlation times of the complexes, (3) the appearance of the ^{31}P NMR spectra in these complexes is determined by the magnitudes and fluctuation times of the cobalt electric field gradients and the ^{59}Co–^{31}P spin–spin couplings, and (4) as the exocyclic group in a monocyclic phosphite ligand is enlarged in these complexes, a decrease of ^{59}Co–^{31}P spin–spin coupling constants accounts for the observed ^{31}P NMR line shapes.

Experimental Section

All cobalt complexes discussed were prepared as BF_4 salts as previously described.[15] Cobalt-59 (70.85 MHz), phosphorus-31 (121.51 MHz), and carbon-13 (75.47 MHz) NMR spectra were recorded on a Bruker WM-300 spectrometer operating in the pulse Fourier transform mode while locked on the ^2H resonance of deuteriated solvents. The T_1 relaxation times were measured by the inversion recovery technique as described by Becker[14] on nondegassed 0.1 M solutions in CD_3CN. The T_1 measurements were reproducible to ±10%.

Results and Discussion

^{59}Co Relaxation Times. In Table I we list ^{59}Co T_1 values and line widths for the series of $[CoL_6]^{3+}$ complexes studied here. When L is a monocyclic phosphite ester, the ^{59}Co T_1 values are an order of magnitude smaller than in the analogous complexes

(1) Operated for the U.S. Department of Energy by Iowa State University under Contract No. W-7405-Eng-82.
(2) Present address: Département de Chimie, Faculté des Sciences, Université de Sherbrooke, Sherbrooke, Québec J1K 2R1, Canada.
(3) Harris, R. K.; Mann, B. E. *NMR and the Periodic Table*; Academic: London, 1978; Chapter 8.
(4) Weiss, R.; Verkade, J. G. *Inorg. Chem.* **1979**, *18*, 529.
(5) Socol, S. M.; Verkade, J. G., to be submitted for publication.
(6) Au-Yeung, S. C. F.; Buist, R. J.; Eaton, D. R. *J. Magn. Reson.* **1983**, *55*, 24 and references therein.
(7) Doddrell, D. M.; Bendall, M. R.; Healy, P. C.; Smith, G.; Kennard, C. H. L.; Raston, C. L.; White, A. H. *Aust. J. Chem.* **1979**, *32*, 1219.
(8) Rose, K.; Bryant, R. G. *J. Magn. Reson.* **1979**, *35*, 223.
(9) Russell, J. G.; Bryant, R. G. *J. Phys. Chem.* **1984**, *88*, 4298.
(10) Chacko, V. P.; Bryant, R. G. *J. Magn. Reson.* **1984**, *57*, 79.
(11) Rose, K. D.; Bryant, R. G. *Inorg. Chem.* **1979**, *18*, 1332.
(12) Ader, R.; Lowenstein, A. *J. Magn. Reson.* **1971**, *5*, 248.
(13) Saito, T.; Sawada, S. *Bull. Chem. Soc. Jpn.* **1985**, *58*, 459.
(14) Becker, E. D. *High-Resolution NMR Theory and Chemical Applications*, 2nd ed.; Academic: New York, 1980.
(15) Socol, S. M.; Verkade, J. G. *Inorg. Chem.* **1986**, *25*, 2658.

0020-1669/87/1326-3221$01.50/0